ECRONICON OPEN ACCESS

EC CARDIOLOGY
Research Article

Impeller Design Analysis and Evaluation of BSRM Total Artificial Heart: Sai Spandan

Pradeep Kumar Radhakrishnan[1]*, Sujatha Mohanty[2], MVKV Prasad[1], Pulivarthi Nageshwar Rao[1], Siva Krishna Rao GV[1], Dorai Nagaraju[1], Nagesh Kumar[1], Bisoi AK[2], Siva Prasad[1], Satya Narayana Murthy[1], Satya Narayana MRS[1], Ravi Shankar[1], Srinivas[1], Das PK[3], Valluvan Jeevanandam[4] and Venugopal P[2]

[1]Gitam University, India

[2]AIIMS, India

[3]IIT Kharagpur, India

[4]University of Chicago, USA

***Corresponding Author:** Pradeep Kumar Radhakrishnan, Professor, Division of Cardiothoracic and Vascular Surgery, GIMSR Gitam University, India.

Received: June 25, 2020; **Published:** August 11, 2020

Abstract

Multiple impeller designs are available for total artificial heart design. Design of centrifugal pumps should minimise shear stress that is cause of haemolysis and thrombosis. The design chosen for impeller of Saispandan is backwardly curved four bladed designs. The impellers are powered by twin 12/14 bearing less switched reluctance motor powering its core. It is a twin motor double impeller assembly with proposed separate control systems for the right and left side. The development envisages in addition to a unique impeller design an automatic speed control system, automatic right/left balance, minimal hemolysis achieved with elegant designing of its elements and analysis using computational fluid dynamics. No thrombogenic zones were noted on analysis.

Keywords: *Saispandan; Hybrid Bearing Less Switched Reluctance Motor; Computational Fluid Dynamics; Centrifugal Blood Pumps; Haemolysis; Thrombosis; Shear Stress*

Introduction

Heart failure causes about 3 - 5,00,000 deaths each year and 20% die waiting for a transplant. Saispandan with twin impellers and double motor design would soon be a hope for future destination therapy in the area of total artificial heart. Saispandan is a fully implantable total artificial heart being designed for destination therapy is in its bench work prototype design stage. 6 cm in diameter and 10 cm in length has a priming volume of 35 ml and it is fully implantable within the chest. The inflow cuffs are anastomosed to the atria and left and right outlet grafts are anastomosed to the ascending aorta and pulmonary artery, respectively. Driven by twin hybrid bearingless switched reluctance motors this device replaces the ventricles of the heart and delivers blood flow to both the systemic and pulmonary circulations. Separate and automatic speed control system for right and left heart with automatic balancing is envisaged for the system.

Pump design

Simple design with acceptable cost materials and unique design with separate controls for both circulations and impellers with variable speed controls providing pulsatile flows are quite unique to the system creating twin pumps at opposite ends of the shaft with a central battery or power chamber. Rotating assembly is 6 cm in diameter by 12 cm in length.

Modelling and evaluation

Two 12/14 hybrid bearingless switched reluctance motors power the impellers separately and they are housed in the central portion of the device. Saispandan is self-regulating, with an inlet pressure-balancing sensor regulator system. Speed variations make it pulsatile and this gives additional parameter of physiologic control. Impeller blade design minimises shear stress and maintains stable operation. Specialised titanium coating induces neointimal lining and gives rise to near normal flow patterns and shear stress identical to a normal endothelial lined heart. There is no central shaft movement and preload adjusts after load for both the pumps. Speed auto-regulation incrementally lowers pump speed in response to suction detection. Valves, sensors, actuation mechanisms, or flexible blood-pumping elements are thereby avoided. Automatic speed algorithm systems use system self-regulation and performance which was tested against a fixed-speed mode, 25% modulated speed mode, and automatic mode using a mock circulatory loop. The sensorless automatic speed control system adjusts the pump speed to maintain a target flow, depending on calculated systemic resistance. This is evaluated in a range of hemodynamic conditions. Hemolysis evaluation is done using bovine blood at a fixed mean speed of 3,400 rpm with a flow of 6.5 L/min and a fixed mean speed of 2,000 rpm with a flow 3.6 L/min and also at a mean speed 2,700 rpm and flow of 5 L/min with a 25% modulated speed mode to produce pulsatile blood flow. A normalized index of hemolysis (NIH) is then adopted to compare the hemolysis properties of each pump.

Methodology

In the present work the pump impeller is made from biocompatible material with vanes undercut deep inside the impeller. Flow simulation of the centrifugal pump with biocompatible impeller made of different materials using CFD was performed. Three different biocompatible materials like polytetrafluoroethylene (PTFE), titanium and stainless steel will be used for impeller.

Geometry modelling and meshing

The computational domain of blood pump consists of four impeller blades with casing, blood inlet and outlet pipes. Three-dimensional computational domain of impeller geometry is created in ICEM CFD 15.0 software. ICEM CFD is an engineering software tool which provides geometry tools and mesh generation tools. The dimensions of geometry are blood inlet diameter of 19 mm, outlet diameter of 27 mm, impeller diameter of 55 mm and blade thickness is 25 mm. the clearance between casing top and blade is given as 1.5 mm. All parts of impeller are specified with appropriate names and boundary conditions of computational domain are identified as well which is presented in figure 1. Further unstructured meshing is chosen for mesh generation since the 3D geometry has sophisticated nature. Firstly, the complete geometry is meshed with the maximum element size of 2 mm and element type of tetrahedrons as shown in figure 2. Later, prism layers were created using exponential law with 10 layers near the solid boundaries such as four blades and impeller casing. These prism layers are useful to study the typical blood flow behaviour which is essential for the design of impeller blade shape as well. It is important to confirm the quality of mesh for the prediction of accurate results. The orthogonal quality is verified for all part of 3D impeller and it is obtained as 0.7. Moreover, the cut section view of meshed geometry is obtained to identify the unmeshed parts of geometry as presented in figure 3. The meshing details of all parts and materials used in the present study are presented in table 1 and 2.

Numerical solution

Three-dimensional computational domain (impeller) unstructured mesh is imported into a computational fluid dynamics (CFD) FLUENT 15.0 software. Governing equations of computational domain both continuity and momentum equations will be solved using finite volume method (FVM) in FLUENT 15.0. In the current study the blood behaviour is assumed as Newtonian incompressible and laminar flow through the impeller. The blood flow inlet at the eye of impeller is 5 l/min and pressure outlet is specified at outlet. Four backwardly directed blades will be rotated with three different constant speeds 2000 rpm, 2500 rpm and 3000 rpm for three different materials steel, titanium and polytetrafluoroethylene (PTFE). Remaining solid walls are specified as no-slip boundary condition.

Governing equations are discretized using finite volume method (FVM) and pressure velocity coupling was performed by using the semi-implicit method for pressure linked equation (SIMPLE) algorithm. Convergence criterion is set for both continuity and momentum

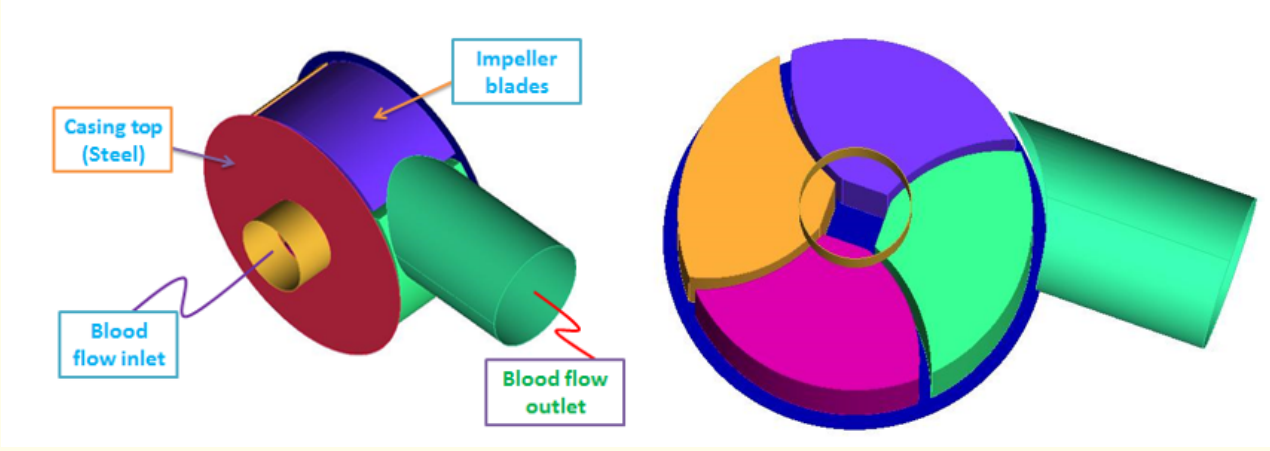

Figure 1: *Three dimensional geometry of impeller with four blades.*

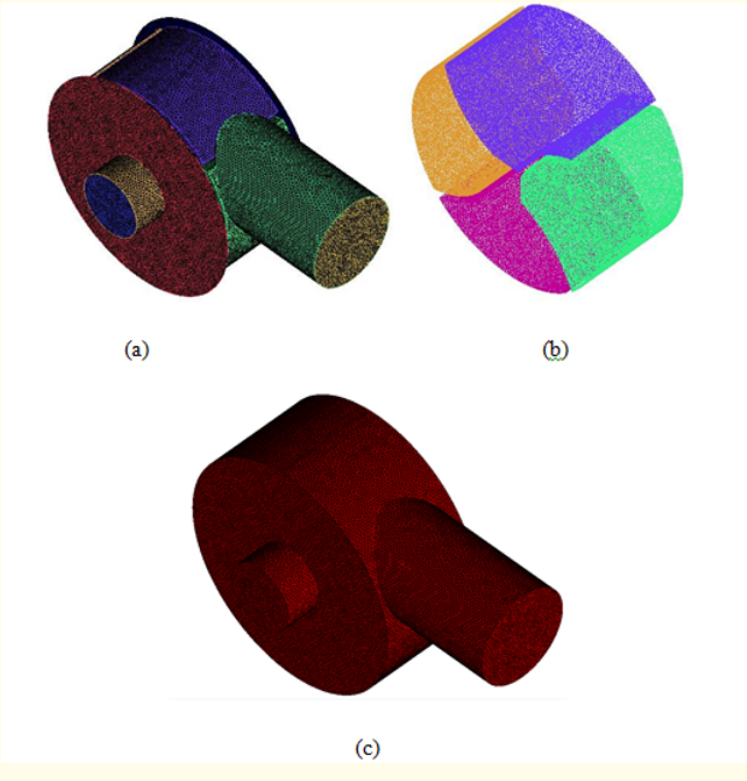

Figure 2: *Meshing of computational domain (a) All parts (b) Four blades (c) Blood flow domain.*

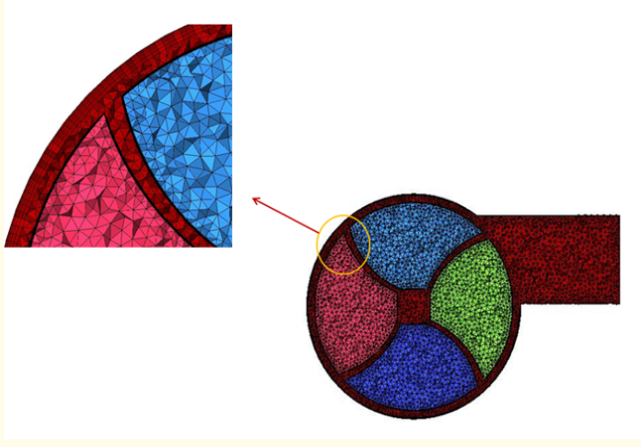

Figure 3: *Prism layer creation near the solid boundary wall.*

Body part	Elements
Blade-1	11342
Blade-1 (Body)	138128
Blade-2	11257
Blade-2 (Body)	137100
Blade-3	11492
Blade-3 (Body)	140275
Blade-4	11323
Blade-4 (Body)	138932
Casing-Bottom	16222
Casing-Top	6634
Fluid	613115
Inlet	718
Inlet-Pipe-Outer	1717
Outlet	1565
Outlet-Pipe-Outer	8442
Total	1256900

Table 1: *Mesh details of 3D impeller.*

Property	Blade material			Blood
	Steel	Titanium	PTFE	
Density (kg/m^3)	8030	4850	2200	1060
Viscosity (kg-m/s)	-	-	-	0.0035

Table 2: *Material details of blood pump.*

as 1E-06. The influence of impeller blade material for different speeds on steady laminar blood flow is analyzed in terms of velocity and pressure contours. The parameters considered in the present study are presented in table 3.

Parameter	Value
Speed (rpm)	2000, 2500, 3000
Clearance gap (mm)	1.5
Blood flow rate (L/min)	5
Blade material	Steel, Titanium, PTFE

Table 3: *Parameters investigated for impeller design.*

Results and Discussion

The relationships between functions of motor power and speed, systemic flow, and systemic vascular resistance (SVR) support sensorless speed control algorithm with advanced controllers. Calculated systemic flow and SVR co relates well with measured pump flow and SVR. Four bladed backward impellers could generate head pressure and flow rate at human body conditions, 80 - 120 mmHg and 5 Liter/min. From a simulation results, almost of shear stress from the impeller and the housing were less than 100 and 200 pa respectively. Housing of backward impeller had the most appropriate shear stress because 98% of shear stress was less than 300 pa. The automatic system adjusts pump's speed to obtain the target flow against the calculated SVR. Atrial pressure difference is maintained within ± 10 mm Hg for a wide range of SVR/PVR ratios, demonstrating a wide margin of self-regulation under fixed-speed mode and 25% sinusoidal modulated speed mode. Blood pump consists of four impeller blades for which three different materials steel, titanium, PTFE were considered at various speed 2000 rpm, 2500 rpm and 3000 rpm. The present analysis is carried out with blood flow 5 L/min at inlet pipe and its behaviour assumed as Newtonian [1-5]. The simulations for three different solid materials at various blade speeds separately and their results analysis in terms of velocity contours have been presented. Figure 4 shows the mid plane of blood pump velocity contours for steel blade at different speeds. It can be seen that maximum velocity of blood within the impeller increased with blade speed. The maximum velocity for blade speed 2000, 2500 and 3000 rpm are 0.95 m/s, 1.2 m/s and 1.4 m/s respectively has been observed. Moreover, the blood flow through the impeller is represented with uniquely coloured velocity path lines and vectors for different blade materials and speeds [6-9]. It is observed that blood flow path has not formed any stagnation zones and significant eddies at constant blade speed. The blood flow path lines and velocity vectors at 3000 rpm steel blade speed is presented in figure 5. Further, comparison of velocity contours for three different blade materials was carried out to predict the optimum solid material for impeller. It is found that blood maximum speed for both steel and PTFE is observed to be same which is approximately 1.4 m/s. whereas for titanium material it will be 1.5 m/s. The same presented in figure 6. The pressure head of blood pump at outlet is predicted for various solid materials at different speeds [10-15]. Also, optimum impeller blade material is predicted in terms of attained pressure head at outlet. The comparison of blood's maximum speed and pressure head (mm of Hg) is presented in table 4. The key controlling physical parameter in the CFD modelling was the pump aperture. 10 mmHg static pressure difference, based upon previous whole pump results, was applied to both pumps, blood entering the bearing region was assumed to be at 37°C, and approximately 2 Watts of heat is generated through viscous dissipation, with peak temperature due to viscous dissipation being limited to 0.60°C above the bulk blood temperature. Additional transfer of heat into the blood from conduction and convection of heat generated by electrical losses in the stator winding, approximately 4 Watts, most of which would be conducted away via the large surface areas of the stator housing. With half of the stator losses being conducted through the housing, the analytical estimate of peak fluid film blood temperature rise becomes about 1.5°C, or 38°C for a bulk blood temperature of 37°C. A sudden change in calculated pump flow may indicate an emergency situation, as suction caused by cannula obstruction or sudden volume loss, or pump stoppage should be dealt with by autoregulation of the pump [16-18]. If this decreased flow continues for 3s or more, pump speed immediately decreases at a programmed rate. After the 3s at this "minimal" flow, pump speed gradually returns to the original or programmed recovery speed level if the situation is corrected. If uncorrected at this stage the alarm would continue to appear in the system interface, and the programmed pump speed or target flow would have to be significantly changed to release the atrial suction [20-22].

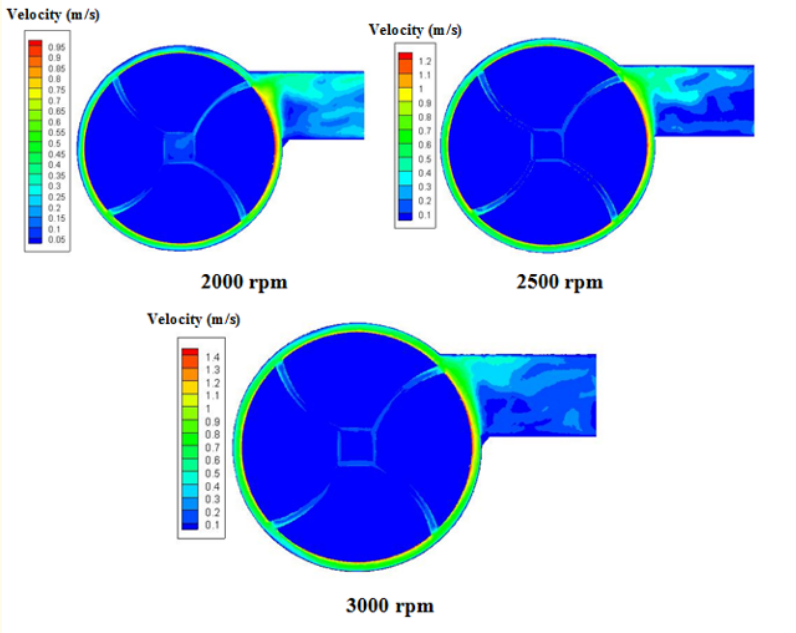

Figure 4: *Velocity contours of impeller mid plane for 5 L/min blood flow rate at 2000, 2500, 3000 rpm speeds.*

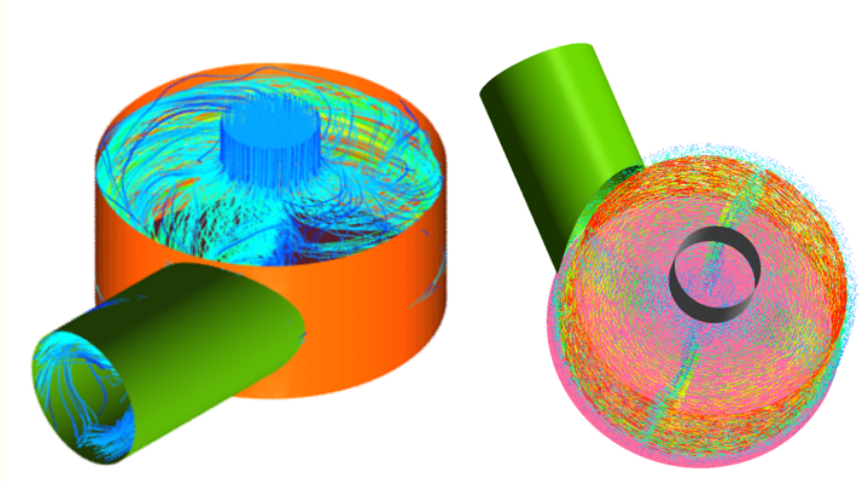

Figure 5: *Uniquely coloured (a) Path lines and (b) Velocity vectors of blood flow in impeller rotating at 3000 rpm.*

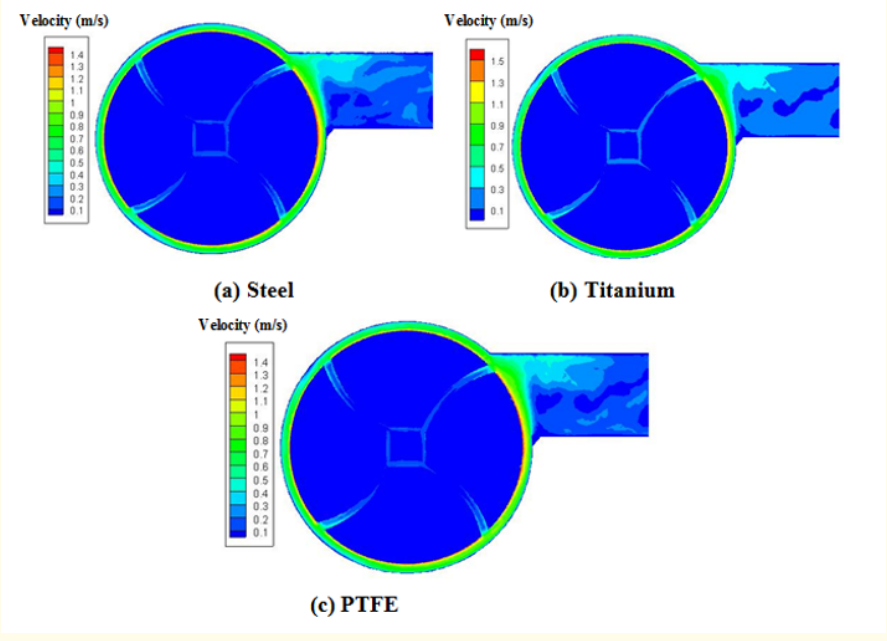

Figure 6: *Velocity contours comparison of three different impeller blade materials at speed 3000 rpm.*

Material	Speed (rpm)	Maximum blood speed in the impeller (m/s)	Pressure head (mm of Hg)
Steel	2000	0.95	75.10
	2500	1.20	95.20
	3000	1.40	105.25
Titanium	2000	1.01	80.15
	2500	1.32	100.15
	3000	1.50	110.25
PTFE	2000	0.98	82.65
	2500	1.25	98.20
	3000	1.45	104.28

Table 4: *Performance comparison of three different blades at various blade speeds.*

Conclusion

The design thus provides hemolysis test results within acceptable values (normalized index of hemolysis <.01 mg/dL) and CFD evaluation showed no thrombogenic zones. Saispandan bearing less total artificial heart with four bladed backward impeller design is the most appropriate impeller for heart pumps because it generates 80 - 120 mmHg and its shear stress was mostly less than 300 pa with results in low hemolysis tendency with no thrombogenic zones. At desired flow rate (5 L/min) and speed more than 2000 rpm, backwardly directed four bladed impellers can generate a head pressure to prevent a suction flow (> 80 mmHg) and a shear stress were less than 300 pa, that makes it the most appropriate design for blood pump due to the least shear stress generation.

Bibliography

1. Guy T." Evolution and current status of the TAH. The search continues". *ASAIO Journal* (1998): 44.
2. Kawahito S., *et al.* "Quantification of pulsatility of the arterial blood pressure waveform during the left ventricular non-pulsatile assistance". *Journal of Congestive Heart Failure and Circulatory Support* (2001).
3. Bohang Zhu., *et al.* "Research on wave energy generation device based on artificial heart pump" (2011).
4. Adkins D and Brennen C. "Analysis of Hydrodynamic Radial Forces on Centrifugal Pump Impellers". *Journal of Fluids Engineering* (1988): 110.
5. Tayama E., *et al.* "The Simple In Vitro Thrombogenic Test: Modified Methods for Same Priming Pumps". *Artificial Organs* (1997): 6.
6. Tsukiya T., *et al.* "Use of motor current in flow rate measurement for the magnetically suspended centrifugal blood pump". *Artificial Organs* (1997).
7. Simaan MA. "Modelling and control of the heart left ventricle supported with a rotary assist device. In Proceedings of the IEEE Conference on Decision and Control". Cancun, Mexico (2008): 9-11.
8. Tsukiya T., *et al.* "Improvement of Washout Flow in a Centrifugal Blood Pump by a Semi-open Impeller". *ASAIO Journal* (2002).
9. Shi Y., *et al.* "Numerical Modelling of Hemodynamics with Pulsatile Impeller Pump Support". *Annals of Biomedical Engineering* (2010).
10. Cheng A., *et al.* "Comparison of continuous-flow and pulsatile-flow left ventricular assist devices: Is there an advantage to pulsatility". *Annals of Cardiothoracic Surgery* (2014).
11. Yamane T., *et al.* "Flow Visualization Measurement for Shear Velocity Distribution in the Impeller-Casing Gap of a Centrifugal Blood" (1999).
12. Yamane T., *et al.* "New mechanism to reduce the size of the mono pivot magnetic suspension blood pump - direct drives mechanism" (1997).
13. Yoshikawa M., *et al.* "Development of the NEDO Implantable Ventricular Assist Device with Gyro Centrifugal Pump" (2000).
14. Yuhki A., *et al.* "Detection of Suction and Regurgitation of the Implantable Centrifugal Pump Based on the Motor Current Waveform analysis and its application to Optimization of Pump Flow" (1999).
15. Xu L., *et al.* "Analysis of a new PM motor design for a rotary dynamic blood Pump". *ASAIO Journal* (1997).
16. Ando M., *et al.* "Electrocardiogram-Synchronized Rotational Speed Change Mode in Rotary Pumps Could Improve Pulsatility". *Artificial Organs* (2011).
17. Tsukiya T., *et al.* "Use of motor current in flow rate measurement for the magnetically suspended centrifugal blood pump". *Artificial Organs* 21.5 (1997): 369-401.
18. Wakisaka Y., *et al.* "Intrathoracic and intraabdominal wall implantation of a centrifugal blood pump for circulatory assist". *Artificial Organs* (1998).
19. Watterson PA., *et al.* "Ventr Assist Hydrodynamically Suspended Open, Centrifugal Blood Pump". *Artificial Organs* (2000).
20. Vandenberghe S., *et al.* "Effect of rotary blood pump failure on left ventricular energetics assessed by mathematical modelling". *Artificial Organs* 26.12 (2002): 1032-1039.

21. Timms DL., *et al.* "Flow Visualization of a Centrifugal Blood Pump". World Congress on Medical Physics and Biomedical Engineering (WC2003), Sydney, Australia (2003).

22. Wampler R., *et al.* "A Seamless Centrifugal Blood Pump with Passive Magnetic and Hydrodynamic Bearings". *Artificial Organs* 23.8 (1999): 780-784.

23. Uriel N., *et al.* "Device thrombosis in HeartMate II continuous-flow left ventricular assist devices: a multifactorial phenomenon". *The Journal of Heart and Lung Transplantation* 33.1 (2014): 51-59.

Volume 7 Issue 9 September 2020